

Anchorage Bond Strength of Glass Fibre Polymer Reinforced Concrete with Palm Kernel Shells as Partial Coarse Aggregate

Authors' contributions

This work was carried out in collaboration among all authors. All authors read and approved the final manuscript.

ABSTRACT

In recent years, the use of GFRP reinforcing bars in place of steel reinforcing bars in concrete structures such as, buildings, roads, and bridges cannot be overlooked as they offer advantages such as higher tensile strength, corrosion resistance, reduced weight and cost effectiveness compared to steel reinforcing bars. The use of PKS as partial coarse aggregate in steel reinforced concrete has been studied by several researchers and found to produce lightweight concrete and reduce construction cost but, the application of GFRP reinforcing bars in LWC such as PKSC, presents a unique structural material with possibly different mechanical and structural properties which requires further studies and this study specifically focused on determining the anchorage bond strength of Glass Fibre Polymer reinforced concrete with PKS as partial coarse aggregate since the bond strength between concrete and reinforcing bars is a crucial prerequisite for the design of reinforced concrete as a composite material. Normal weight concrete of mix ratio 1:1.5:3 with water-cement ratio (w/c) of 0.5 and lightweight concrete with 10% of the volume of coarse aggregate replaced by PKS were used in a total of forty-eight (48) double pull-out prismatic specimens of dimension 100mm x 100mm x 300mm for control and test specimens respectively, embedded with 12mm and 16mm diameter GFRP reinforcing bars at varying end-to-end embedment lengths (100mm, 125mm and 150mm) and 300mm continuous embedment. Average anchorage bond strength of 4.684N/mm² and 3.558N/mm² were respectively recorded for the PKSC with 12mm and 16mm diameter bars and 100mm embedment length and 3.051N/mm² and 2.899N/mm² respectively for PKSC specimens with 12mm and 16mm diameter bars and 150mm embedment length, indicating a decrease in anchorage bond strength with increasing (end-to-end) embedment length. However, the highest average anchorage bond strength of 6.174N/mm² and 4.581N/mm² were respectively recorded for PKSC specimens with 12mm and 16mm GFRP reinforcing bars and continuous (300mm) embedment length. Comparatively, the average percentage anchorage bond strength values ranging between 75.5-97.9% of that of NWC were recorded for PKSC and an increase in GFRP reinforcing bar diameter resulted in a decrease in anchorage bond strength. Splitting failure was observed for most of the specimens with longitudinal and transverse crack patterns developed

after load application regardless of the size of GFRP reinforcing bar or concrete mix but the extent and visibility of the cracks formed reduced in specimens with continuous bar embedment.

Keywords: Reinforced Concrete; GFRP; Palm Kernel Shells; Anchorage Bond Strength; Partial Coarse Aggregate.

1. INTRODUCTION

Most structures are built using concrete which is a mixture of cementitious material, aggregates and water. Occasionally, an extra substance called an admixture is added to change certain properties for certain uses [1]. According to Chandra and Berntsson[2], studies have been carried out to find ways to partially or completely replace the conventional aggregates especially coarse aggregates in concrete in order to produce lightweight concrete, lower construction costs and reduce the rate of environmental degradation. Therefore, numerous research on the use of palm kernel shells (PKS) as LWA to replace NWA in structural elements and road construction in Southeast Asia and Africa have been conducted over the last 27 years [3]. The low tensile strength but high compressive strength of concrete requires the introduction of steel reinforcing bars which have high tensile strength in the tension zone of the concrete section to act compositely. In steel reinforcement, corrosion is a chemical process that produces chemicals that damage the bond between steel reinforcing bars and concrete, decreasing bond strength and ultimately limiting the service life of reinforced concrete structures [4]. In nations like the US and Canada, this issue eventually results in a significant financial burden during routine maintenance, repairs and rehabilitation[5]. Therefore, the use of GFRP as an alternative solution to the deterioration of civil infrastructures like bridge decks, tunnels, roads and other specialized concrete constructions is due to its advantages over steel reinforcement including higher tensile strength, corrosion resistance, lighter weight and cost effectiveness [6, 7]. The most crucial prerequisite for the design of reinforced concrete as a composite material, is the efficacy of the bond strength between concrete and reinforcing bars which can be ascertained in a few different ways[8]. The ordinary pull-out test, push-out test, beam test and double pull-out test are a few of

these tests. By measuring the force needed to remove the reinforcing bar that has been placed into the concrete specimen, the most popular test for determining the bond strength between concrete and steel reinforcing bar is the ordinary pull-out test which according to Bickley [9], was not thought of as a workable site method until the 1970s. However, the results of the ordinary pull-out test method, tend to be overestimated and does not depict the true bond strength of the concrete-reinforcing bar interface in the tensile zone as the concrete is subjected to compression while the steel bar is under tension [10]. Another pull-out test technique called the double pull-out test provides more precise bond strength results because it simulates the behavior of a beam tensile stress zone by putting tension on both the steel rebar and the concrete. Concrete reinforced with GFRP reinforcing bars and PKS as partial coarse aggregate presents a unique structural material with possibly different mechanical and structural properties but currently, no empirical studies exist that describe these properties specifically, the bond strength between PKSC and GFRP reinforcing bars. Therefore, undertaking this study is necessary to fill the knowledge gap by investigating the anchorage bond strength of Glass Fibre Polymer reinforced concrete with PKS as partial coarse aggregate. The effect of bar size, effect of embedment length, bond failure mechanism, among other properties were investigated. However, based on previous studies by [10-14], this study was limited to 10% PKS replacement of coarse aggregate as further increase in the PKS content in concrete would result in a decrease in the anchorage bond strength and consequently, affect structural safety.

2. PREVIOUS STUDIES

2.1 PKS Content in Concrete

Gupta et al. [11] studied the partial replacement of coarse aggregates with PKS at rates of 10%, 13%, 15%, 20%, and 25% in concrete by testing the compressive strength of 150 mm x 150 mm x 150 mm cubes which were cast with mix ratio, 1:1.5:3 by volume batch. Results showed that 10% partial replacement was optimum without compromising on the compressive strength of concrete. Odeyemi et al. [12] investigated the bond strength between high yield steel reinforcing bars and partially replaced Self Compacting PKS concrete in which 50% of the granite content of the concrete was substituted with palm kernel shells. It was determined that PKS could be safely used for partial replacement in SCC.

Olanipekun et al. [13] studied the mechanical properties of PKS using 1:1:2 and 1:2:4 mix ratios with 0%, 25%, 50%, 75% and 100% PKS replacement. They reported a reduction in the compressive strength with increasing PKS content and Alengaram et al. [14] compared the bond properties of PKSC with NWC and reported that the bond strength of PKSC was 86% of that of NWC.

Alengaram et al. [15] after reviewing previous research works on the use of palm kernel shells (PKS) as lightweight aggregate (LWA) concluded that, PKSC operates structurally and mechanically equivalent to normal weight concrete (NWC).

2.2 Bar Size and Embedment Length

The diameter or bar size and the length of reinforcement required to be embedded in concrete to obtain the full bond strength between concrete and reinforcement, both affect the bond strength of concrete. Buabin et al. [10] studied the bond strength of steel reinforcing bars locally milled from scrap metals in concrete prepared with PKS as coarse aggregate by considering four concrete mixes with varying PKS contents of 0%, 25%, 50% and 100% in double pull-out prismatic specimens and embedded with 12mm and 16mm diameter steel reinforcing bars. The maximum anchorage bond strength of 10.13 N/mm^2 and 7.26 N/mm^2 were recorded for the NWC and with 12mm and 16mm diameter steel reinforcing bars respectively. However, 25% PKS replacement resulted in a reduction of the bond strength to 8.52 N/mm^2 and 6.82 N/mm^2 respectively for 12mm and 16mm diameter steel reinforcing bars and even further decrease up to 4.41 N/mm^2 and 3.63 N/mm^2 respectively for 12mm and 16mm diameter steel reinforcing bars at 100% PKS replacement, indicating a decrease in anchorage bond strength with increase in bar diameter and PKS percentage replacement.

More recent study by Boateng et al. [16] looked at the bond characteristics of concrete produced from PKS-waste automobile tire aggregates and embedded with deformed mild steel reinforcing bars. Concrete cubes (150mm x 150mm x 150mm) were cast with varying PKS-tire content of 0%, 25%, 50% 75% and 100% and with steel bars of embedment lengths 75mm and 150mm. Pull-out test was carried out to evaluate the bond strength between the steel and the various concrete mixes and the values recorded were up to 8.01 N/mm^2 and 5.98 N/mm^2 for bar sizes 12

mm and 16 mm respectively indicating an increase in bar size and embedment length results in a reduction in the bond stress.

Wang et al.[17] investigated the bond performance between GFRP bars and concrete by considering the effects of three (3) different GFRP bar surface treatments and embedment lengths. The results of the study indicated a decrease in bond strength with increase in bar size and embedment length which was attributed to the gradual transfer of the bond stress during the pull-out test from the loaded end to the free end, resulting in a nonlinear stress distribution of the bond stress along the embedment length of GFRP bar[18-20].

2.3 Bond Behavior and Mechanism of GFRP Bars in Concrete

It is important to better understand the bond behavior and mechanism of GFRP bars in concrete structures for more widespread applications. Shahidi et al.[18] looked into the long-term performance of FRP and how sustained loading affected the bond between concrete and FRP bars. One type of GFRP, two types of Carbon FRP and conventional steel reinforcing bars were tested statically to failure and under sustained loads in pull-out specimens with different embedment lengths and the short-term bond strengths of FRP bars were found to be lower than those of steel. Yan et al. [19] conducted a review on the bond mechanism and bond strength of GFRP bars in concrete, summarizing the results from previous studies primarily on bond mechanism in terms of failure modes and bond strength. 682 pull-out test specimens were mined from previous literature and a comprehensive statistical study was conducted. All the data supported that pullout and splitting failures are overwhelmingly dominant over all of the failure modes. They also identified that bond strength has linear relationships with concrete compressive strength and bar size and there is a nonlinear relationship between the bond strength and embedment length. Ifrahim et al. [20] examined the effects of bar material, diameter and embedment length on the bond strength of steel and GFRP bars by using twelve (12) 200mm x 200mm x 200mm cube specimens. It was found that the bond strength of GFRP bars in concrete decreased with an increase in bar diameter and embedment length. The bond strength of GFRP bars was 42% less than that of steel reinforcement.

Tang [21] studied the uniaxial bond stress-slip characteristics of reinforcing bars in concrete with different compressive strengths and reported that the maximum value on the stress distribution curve mainly occurred at or near the central anchored point, whereas the minimum value occurred at the loaded end due to the symmetry. Also, the bond stress-slip relationship varied with the position of the reinforcing bar and the closer the stress was to the center of the specimen, the steeper the curve became and the more the bond stiffness increased. The review of previous studies by Yan et al. [19] also identified pullout and splitting failures for GFRP bars embedded in concrete as the two major failure modes accounting for over 80% of all the failure modes of irrespective of concrete mix and compressive strength. Diab et al. [22] described splitting bond failure as extremely sudden and brittle due to the rapid production of longitudinal splitting cracks and development of the transverse crack which can be attributed to the matrix-tension failure through the net concrete section at the point of high concrete tensile stress concentration developed at the reinforcing bar end where there is a loss of most of its bond [23-25].

3. MATERIALS AND METHODS

3.1 Materials

The materials used for the study shown in (Fig. 1) included coarse aggregate (granite), fine aggregate, palm kernel shells used as partial replacement of coarse aggregate, ordinary Portland cement, water and GFRP reinforcing bars which are ribbed and sand-coated. The crushed granitic rock used as coarse aggregates had a maximum particle size of 20mm which exceeds and satisfies the minimum coarse aggregate size of 5mm specified by BS 882 [27]. Fine aggregate used was natural sand with maximum particle size of 4.75mm. The aggregates were air dried and kept away from moisture in order to prevent bulking. Palm kernel shells used as partial replacement of coarse aggregates in test specimens were obtained from a local palm kernel oil factory and varied in sizes between 13.20mm and 2mm which is comparable to the study by Alengaram et al. [28]. Cement used was the ordinary Portland cement of weight 50kg and of grade 42.5R from the local market. Clean water devoid of contaminants was used. Glass Fibre Reinforcement Polymer (GFRP) reinforcing bars obtained from a local factory in Tema, Ghana, of actual diameters 12mm and 16mm respectively when measured with a Vernier caliper and

expected minimum tensile strength of 758N/mm^2 as specified by the manufacturer were used in test specimens. Concrete mix ratio of 1:1.5:3 and water-cement ratio (w/c) of 0.5 were used for the normal weight concrete and 10% of the volume of coarse aggregate was substituted by PKS for the concrete with PKS as partial coarse aggregate replacement as determined by Gupta et al.[11] as the optimum PKS content without compromising on the compressive strength of concrete. The measurement of the gravel, sand, cement and PKS were by volume (m^3) and mixed with water measured in litres (ltr). Batching by volume was done because of the relatively low density of PKS compared to granite and would ensure accurate relative proportion of PKS in the mix. The palm kernel shells (PKS) were soaked in water for at least 20 minutes before batching since PKS has higher water absorption rate which has an effect on the workability of concrete and cement hydration [29]. The mixing was done manually on a clean surface.

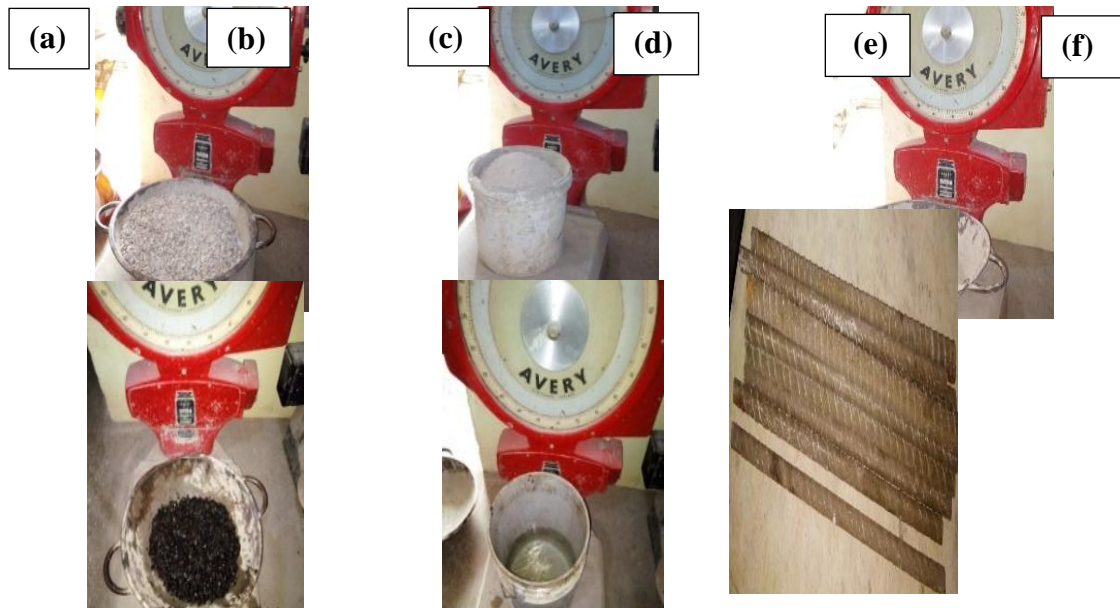


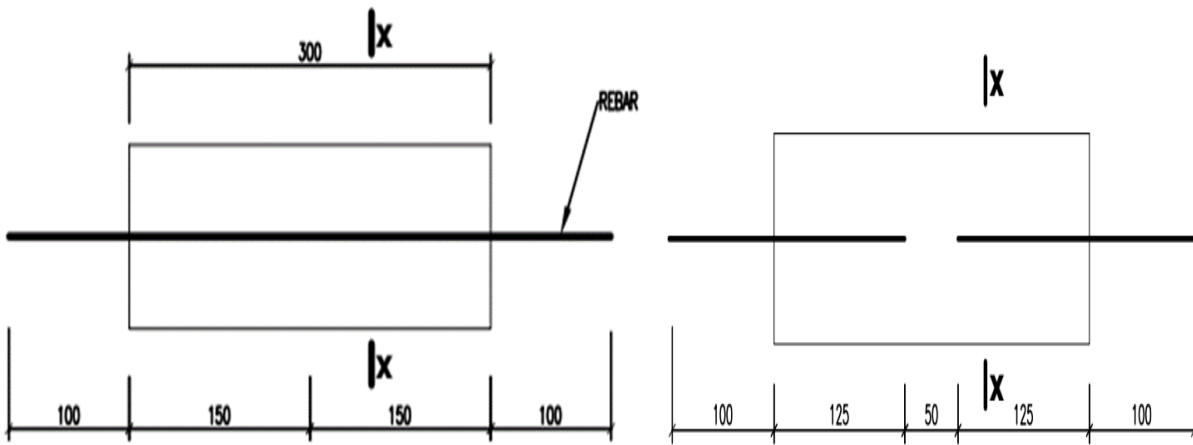
Fig.1: Materials: (a) gravel, (b) sand, (c) cement, (d) PKS soaked in water for 20mins, (e) water (f) cut GFRP bars.

3.2 Specimens

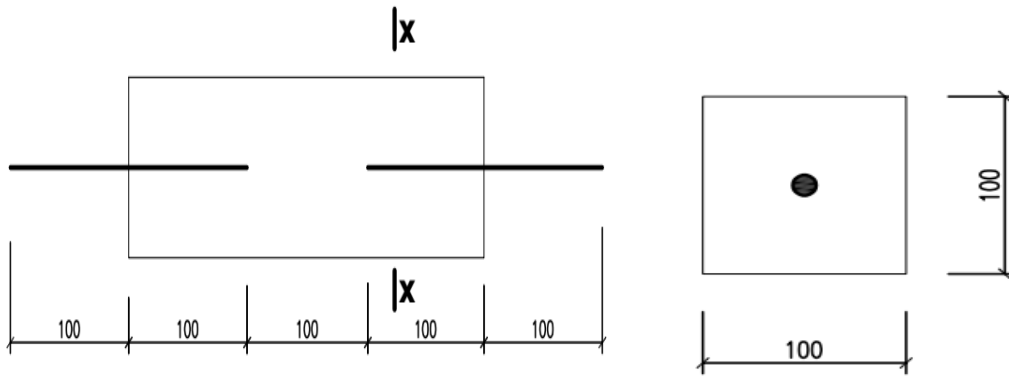
3.2.1 Concrete prism specimens

A total of forty-eight (48) test and control concrete prism specimens of dimension $100\text{mm} \times 100\text{mm} \times 300\text{mm}$ were cast for the anchorage bond or double pull-out test. Three (3) prisms each

were with GFRP reinforcing bars of diameter 12mm and 16mm placed concentrically at varying embedment lengths of 300mm (continuous), 150mm (end-to-end), 125mm (end-to-end) and 100mm (end-to-end) embedment lengths for both test and control specimens respectively with a grip length of 100mm at both ends of each concrete prism as illustrated in (Fig.2) and shown in Figs. 3(a) and (b). The notations of the test and control concrete prism specimens shown in Table 5, imply C-GF12 and C-GF16, represent the control specimens with NWC and GFRP reinforcing bars of diameters 12mm and 16mm respectively. S-GF12 and S-GF16 denote the test specimens with 10% PKS concrete and GFRP reinforcing bars of diameters 12mm and 16mm respectively. The ELS, EL150, EL125 and EL100 suffixes imply continuous, 150mm, 125mm and 100mm embedment length respectively.



(a) (b)



(c)

(d)

Fig. 2: Illustration of concrete prism specimens for double pull-out test:(a) with 150mm rebar embedment (b) with 125mm rebar embedment, (c) with 100mm rebar embedment, (d) section x-x

3.2.2 Concrete cube specimens

Nine (9) concrete cube specimens of dimension 150mm x 150mm x 150mm with 10% PKS as partial coarse aggregate replacement and nine (9) cubes with normal weight concrete were cast to determine their compressive strengths respectively as shown in Fig. 3(d). Three (3) cubes each of the two concrete mixes were used to determine the average compressive strengths after 7 days, 14 days, and 28 days respectively.

3.2.3 Concrete cylindrical specimens

Six (6) concrete cylindrical specimens of dimensions 150mm x 300mm as specified by BS EN 12390-6 [30] were used for the splitting tensile strength test as shown in Figure 3(c). Three (3) specimens were with concrete with 10% PKS as partial coarse aggregate replacement and three (3) specimens with normal weight concrete. Table 4 shows the test specimens with 10% PKSC labelled S1, S2 and S3 and control specimens with NWC labelled C1, C2 and C3.

(a)

(b)



(c)

(d)

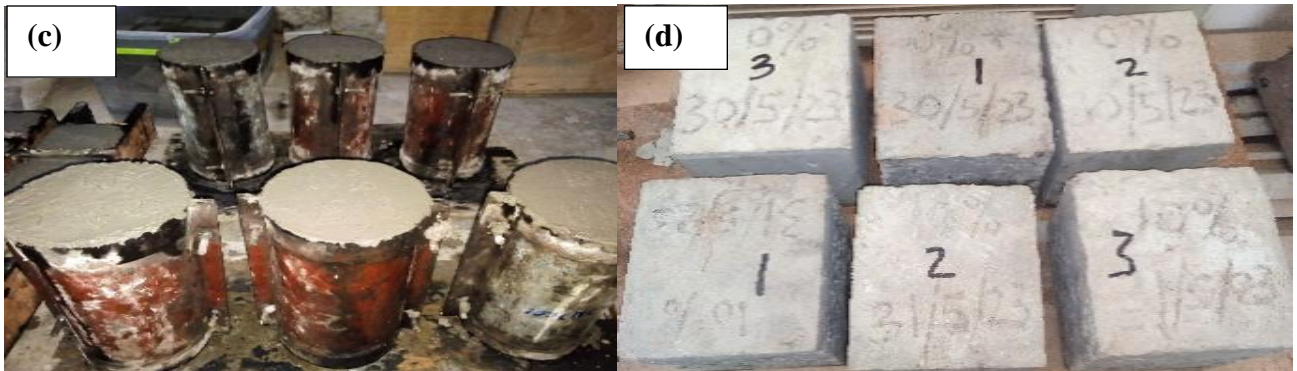


Fig. 3: Specimens: (a) Prism specimens, (b) Hardened prism specimen, (c) cylindrical specimens, (d) cube specimens

3.2.4 Tensile test specimens

Three (3) pieces of each of the GFRP reinforcing bars of actual diameters of 12mm and 16mm were measured with Vernier calipers and cut in lengths of 600mm to determine their tensile strength.

3.3 Test Procedure

3.3.1 Tensile test of GFRP

The tensile strength of the GFRP reinforcing bars was determined using the UTM in accordance with ASTM D7205 [31]. To prevent the premature failure at the grips due to stress concentrations at the anchorage points, adequate grip lengths of 150mm were used at the two ends of each specimen in order to allow failure to occur at the middle of the specimen during testing [4]. The two ends of each GFRP specimen were placed in steel tubes of lengths 150mm and thickness of 3mm. The steel tubes had internal diameters of 16mm and 25mm to provide adequate space for the epoxy resin fill to ensure adequate bond with the GFRP reinforcing bar specimens of diameters 12mm and 16mm respectively. They were bonded together with a cementitious grout or epoxy resin surrounding the bar and allowed to dry for 2 days. The specimens were then placed in the upper and lower jaws of the UTM and an extensometer attached at the middle of the gauge length to measure the corresponding strains. Tensile force was applied gradually till the ideal failure mode of a GFRP reinforcing bar during tensile test which is the splitting of the bar ends [32]. The maximum tensile strength and corresponding strains of the GFRP reinforcing bar specimens were then recorded and the average determined. Figs. 4(a) and (b) respectively show the preparation of test specimens and the tensile strength test of GFRP reinforcing bar specimens using UTM.

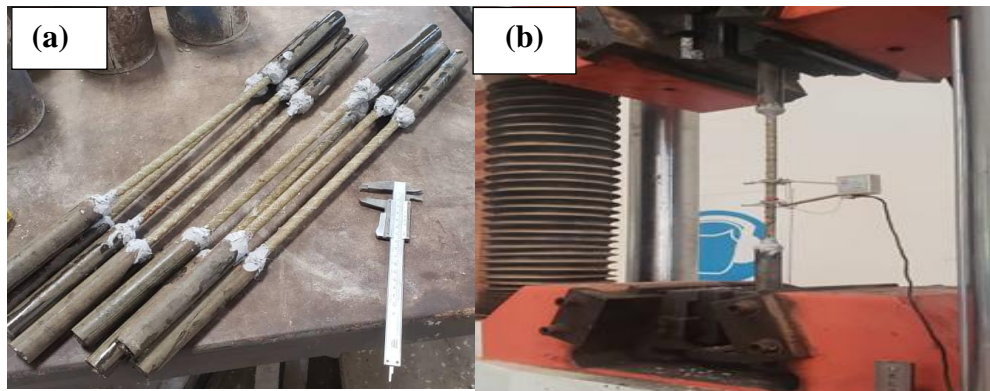


Fig. 4: GFRP reinforcing bar tensile test using UTM: (a) preparation of test specimens, (b) testing.

3.3.2 Anchorage bond test of GFRP

The anchorage bond or double pull-out test was conducted on the 28th day by fixing the two ends of the GFRP reinforcing bars embedded in the test and control concrete prism specimens firmly in position with the metallic wedges in both the upper and lower jaws of the UTM as shown in fig. 5 (a). The GFRP reinforcing bar grips at the ends of the prisms were not held during transportation and before testing in order to prevent any distortions or displacements. The two ends of the specimens were simultaneously pulled in tension until the embedded reinforcing bars lost grip as the bond between the reinforcing bars and the surrounding concrete failed after exceeding the maximum force.

The anchorage bond strength is computed as; $F_b = \frac{P}{\pi dL}$ (1)

Where; F_b = bond stress (N/mm²);

P = maximum applied load (N);

d= nominal diameter of rebar (mm);

L = embedment length of rebar (mm)

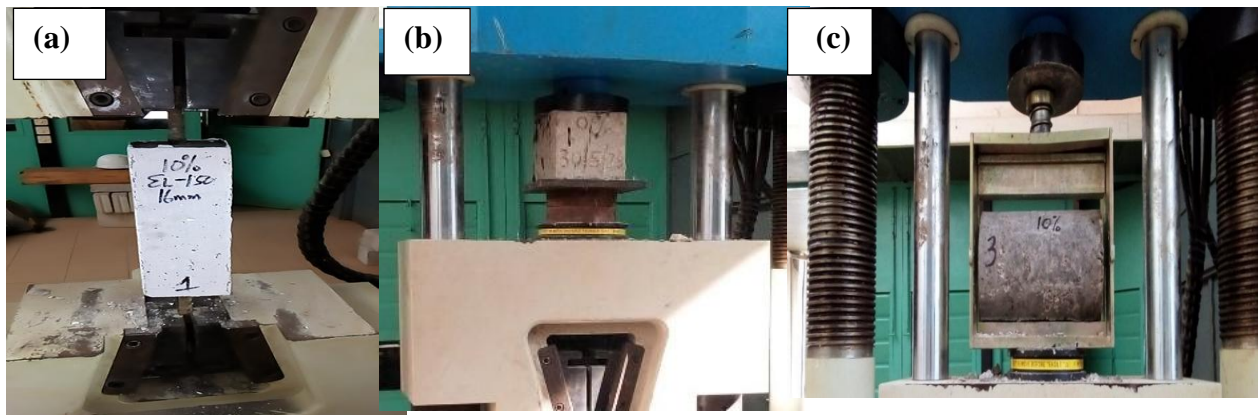


Fig. 5: Testing of specimens using UTM: (a) Anchorage bond strength (double pull-out) test, (b) compressive strength test, (c) splitting tensile strength test.

3.3.3 Concrete Compressive Strength Test

Compressive strength of the cured concrete cubes for both concrete mixes was determined at 7 days, 14 days and 28 days in accordance with BS EN 12390-3 [33], using the UTM as shown in fig. 5(b).

3.3.4 Concrete Split Cylinder Test

Splitting tensile strength was determined according to BS EN 12390-6[30]. The specimens were placed in a steel encasement of internal length 300mm and placed on the middle crosshead of the UTM as shown in fig. 5 (c). Load was then applied to the specimens through the upper crosshead until splitting tensile failure of the concrete occurred.

The splitting tensile strength is computed as:

$$F_{spt} = \frac{2P}{\pi dL} \dots\dots\dots (2)$$

Where; F_{spt} = splitting tensile strength (N/mm²);

P = maximum applied load (N);

L = Length of test specimen (mm) and

d= diameter of specimen (mm)

4. RESULTS

4.1 Slump Test

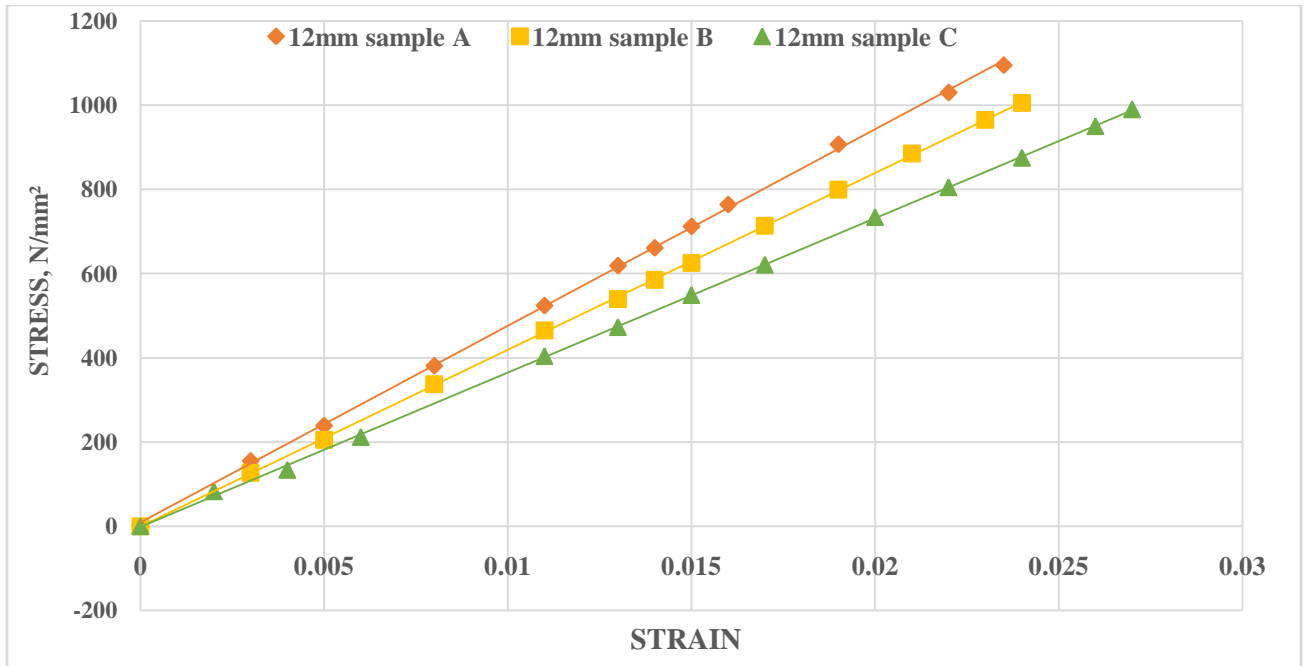
The slump test result for the normal weight concrete ranged from 8mm to 45mm and that of the concrete with 10% PKS was 0mm which is comparable to the very low slump values (0–4 mm) reported by [34-36], indicating very low workability which can be attributed to the high porosity characteristics of PKS used as partial replacement of coarse aggregates. Significant amount of the water used for the batching might have been absorbed by the PKS and consequently, reduced the workability of PKSC.

4.2 Tensile Strength of GFRP

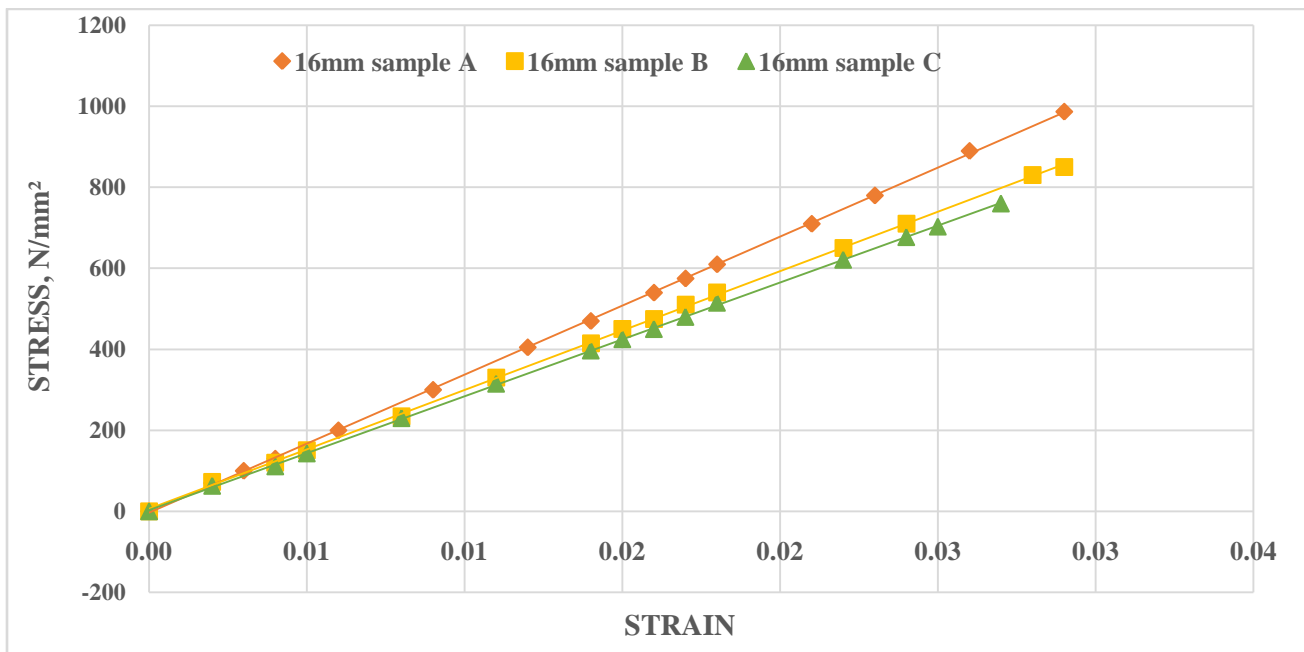
Three samples labelled sample A, B and C respectively for each bar diameter were used for the test and an average tensile strength of 1030 N/mm^2 and maximum strain of 0.0248 were recorded for the 12mm GFRP reinforcing bar and an average tensile strength of 866 N/mm^2 and maximum strain of 0.028 for the 16mm GFRP reinforcing bar shown in Table 1. The average Young's modulus of elasticity recorded were 41.71GPa and 30.52GPa respectively for the 12mm and 16mm GFRP reinforcing bars. These values recorded exceeded the tensile strength and strain values provided by the local manufacturer. Figs. 6 (a) and (b) show the stress-strain curves for the GFRP reinforcing bars of diameter 12mm and 16mm used for the study respectively. Results from the curves indicate an increase linearly throughout their deformations up to the maximum load where failure occurred suddenly [37, 38].

Table 1: Tensile strength test for GFRP reinforcing bars

SAMPLE	NOMINAL DIA., mm	ACTUAL DIA., mm	FORCE (P), N	MODULUS OF ELASTICITY (GPa)	TENSILE STRENGTH, N/mm^2	STRAIN
A	12	12	123844.50	46.43	1095	0.0235
B	12	12	113665.50	42.02	1005	0.0240
C	12	12	111969.00	36.68	990	0.0270
AVERAGE	12	12	116493.00	41.71	1030	0.0248
A	16	16	198446.22	34.10	987	0.0290
B	16	16	170901.00	29.36	850	0.0290
C	16	16	152805.60	28.09	760	0.0270
AVERAGE	16	16	174050.94	30.52	866	0.0280



(a)



(b)

Fig. 6: Stress-strain curve for tested: (a) 12mm diameter GFRP reinforcing bars, (b) 16mm diameter GFRP reinforcing bars

4.3 Concrete Compressive Strength

Cube specimens with NWC had average compressive strengths of 18.07 N/mm², 20.23 N/mm² and 22.25 N/mm² after 7 days, 14 days and 28 days respectively and those with 10% PKS as partial coarse aggregate replacement had average compressive strengths of 10.37 N/mm², 14.36 N/mm² and 15.79 N/mm² after 7 days, 14 days and 28 days respectively indicating a 29% reduction in the 28 days compressive strength for the PKSC. The average compressive strengths of the two concrete mixes are plotted against age in (Fig. 7) and the average 28 days compressive strength of both concrete mixes are shown in Tables 2 and 3 respectively.

Table 2: 28 days compressive strength for 10% PKS concrete

28 DAYS TEST			
Sample	1	2	3
Mass (kg)	7.055	7.117	8.135
Compressive Strength (N/mm ²)	12.79	15.54	19.04
Average Compressive Strength (N/mm ²)	15.79		

Table 3: 28 days compressive strength for normal weight concrete

28 DAYS TEST			
Sample	1	2	3
Mass (kg)	7.944	8.124	7.895
Compressive Strength (N/mm ²)	22.11	23.32	21.34
Average Compressive Strength (N/mm ²)	22.25		

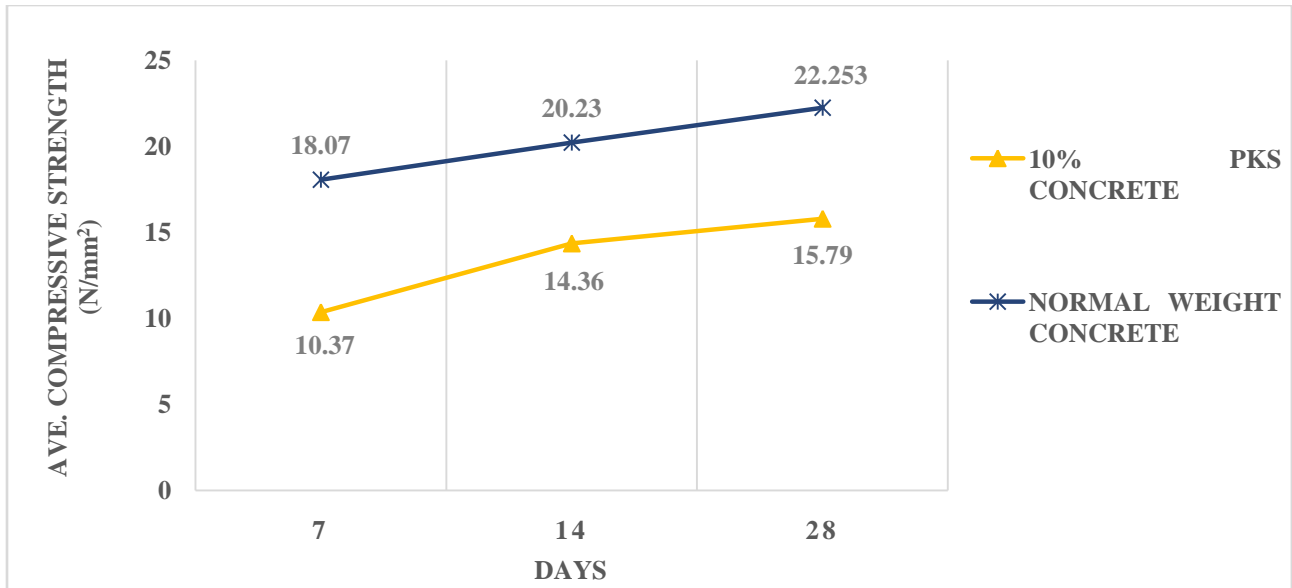


Figure 7: Average compressive strength versus days

4.4 Concrete Splitting Tensile Strength

The average splitting tensile strength value obtained for the NWC using Equation (2) was 2.76 N/mm² and 1.94 N/mm² for concrete with 10% PKS as partial coarse aggregate replacement which indicates a 29.71% reduction and almost comparable to the values (2.0-2.4 N/mm²) obtained by [15, 39]. Table 4 and Fig. 8 show the results of splitting tensile strength test of the NWC and PKSC after 28 days.

Table 4: Splitting tensile strength test

S/No.	SAMPLE	LOAD, P (N)	SPLITTING TENSILE STRESS (N/mm ²)	AVE. SPLITTING TENSILE STRESS (N/mm ²)
	<u>NWC</u>			
1	C1	221704.00	3.14	2.76
2	C2	183073.00	2.59	
3	C3	179542.00	2.54	
	<u>10% PKSC</u>			
4	S1	124849.00	1.77	1.94
5	S2	152155.00	2.15	
6	S3	134779.00	1.91	

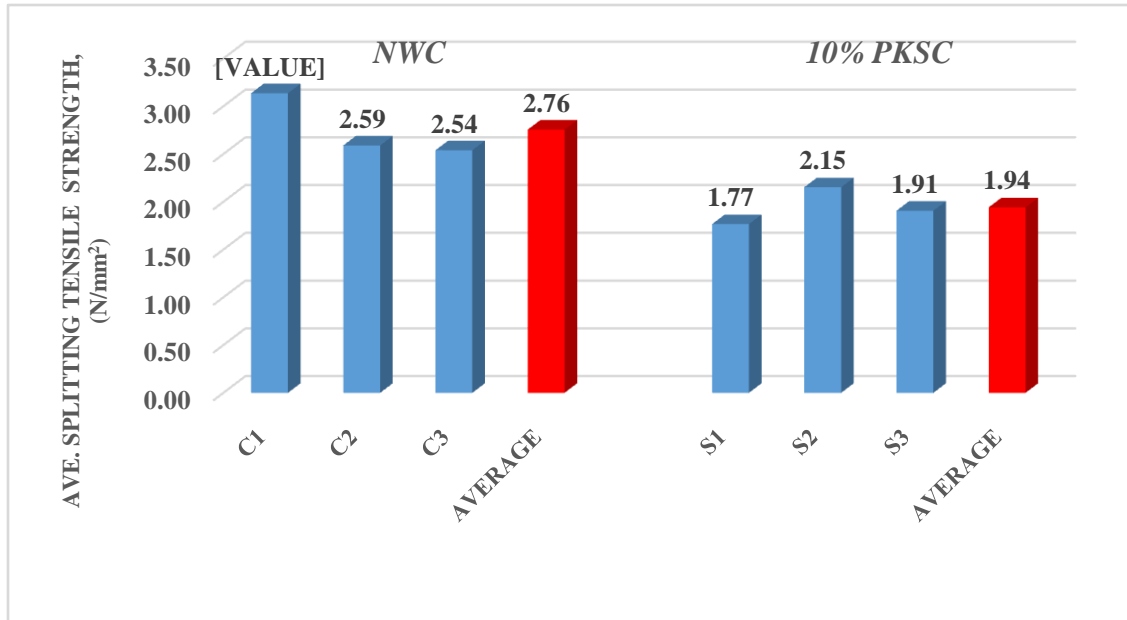


Figure 8: Average splitting tensile strength of normal weight and PKS concrete

4.5 Anchorage Bond Strength

The average anchorage bond strength were computed with Equation (1) and values recorded for the test and control prism specimens with GFRP bars of diameters 12mm and 16mm and various embedment lengths are shown in Table 5 and Fig. 9. The values for the specimens with 300mm (continuous) embedment were obtained by considering half of the length (150mm) based on a study by Tang [21] which indicates that, bond stress–slip relationship varied with the position of the reinforcing bar and the closer the stress was to the center of the specimen, the steeper the curve became and the more the bond stiffness increased. Therefore, the average anchorage bond strength obtained for the test and control specimens with 12mm GFRP bars and 300mm (continuous) embedment were respectively 6.174 N/mm^2 and 6.306 N/mm^2 . The results obtained for the test and control specimens with 16mm GFRP bars and 300mm (continuous) embedment were respectively 4.581 N/mm^2 and 5.584 N/mm^2 . Average anchorage bond strength values of 3.051 N/mm^2 and 3.558 N/mm^2 were respectively recorded for the test and control specimens with 12mm GFRP bars and 150mm (end-to-end) embedment, 2.899 N/mm^2 and 3.198 N/mm^2 were respectively for the test and control specimens with 16mm GFRP bars and 150mm (end-to-end) embedment, 4.464 N/mm^2 and 5.287 N/mm^2 were respectively for the average anchorage bond

strength for the test and control specimens with 12mm GFRP bars and 125mm (end-to-end) embedment, 3.087 N/mm² and 3.259 N/mm² were respectively recorded for the test and control specimens with 16mm GFRP bars and 125mm (end-to-end) embedment, 4.684 N/mm² and 5.592 N/mm² were respectively recorded for the test and control specimens with 12mm GFRP bars and 125mm (end-to-end) embedment and lastly, 3.558 N/mm² and 4.712 N/mm² for the test and control specimens with 16mm GFRP bars and 125mm (end-to-end) embedment.

Table 5: Average anchorage bond strength for test and control prism specimens with GFRP reinforcing bars at varying embedment lengths.

<u>SAMPLE</u>	<u>ACTUAL DIAMETER, (mm)</u>	<u>EMBEDMENT LENGTH (mm)</u>	<u>AVE. ANCHORAGE BOND STRESS (N/mm²)</u>	<u>% AVE. ANCHORAGE BOND STRESS OF NWC</u>
C-GF12-ELS	12	300 (continuous)	6.306	97.901
S-GF12-ELS	12	300 (continuous)	6.174	
C-GF16-ELS	16	300 (continuous)	5.584	
S-GF16-ELS	16	300 (continuous)	4.581	
C-GF12-EL150	12	150 (end-to-end)	3.558	85.750
S-GF12-EL150	12	150 (end-to-end)	3.051	
C-GF16-EL150	16	150 (end-to-end)	3.198	
S-GF16-EL150	16	150 (end-to-end)	2.899	
C-GF12-EL125	12	125 (end-to-end)	5.287	84.424
S-GF12-EL125	12	125 (end-to-end)	4.464	
C-GF16-EL125	16	125 (end-to-end)	3.259	
S-GF16-EL125	16	125 (end-to-end)	3.087	
C-GF12-EL100	12	100 (end-to-end)	5.592	83.759
S-GF12-EL100	12	100 (end-to-end)	4.684	
C-GF16-EL100	16	100 (end-to-end)	4.712	
S-GF16-EL100	16	100 (end-to-end)	3.558	

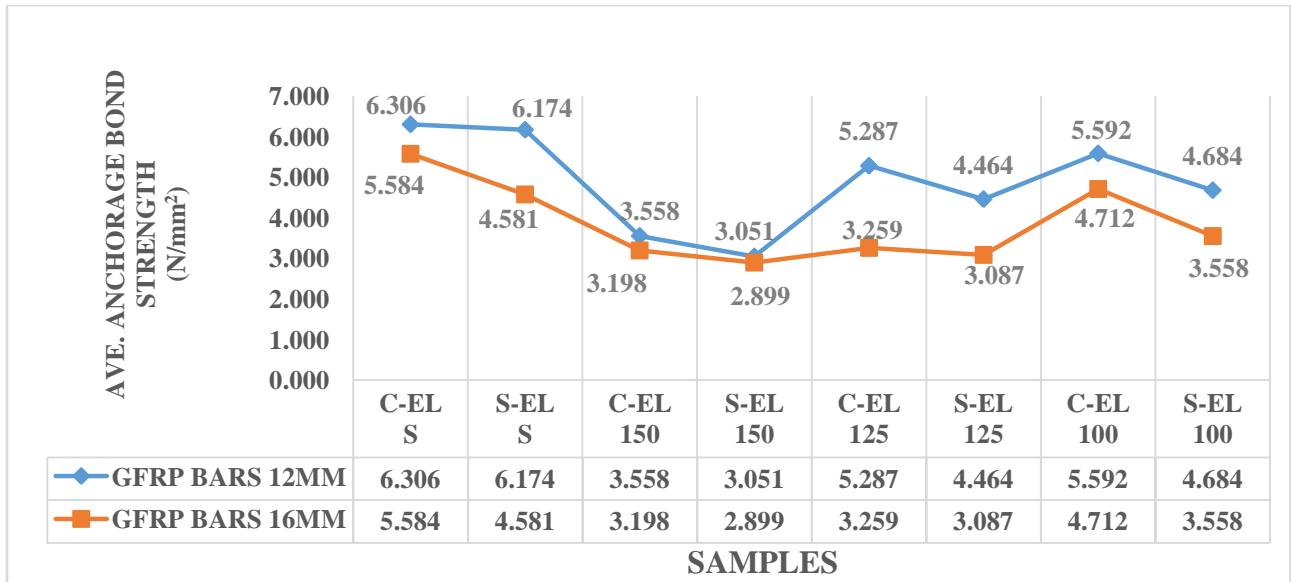
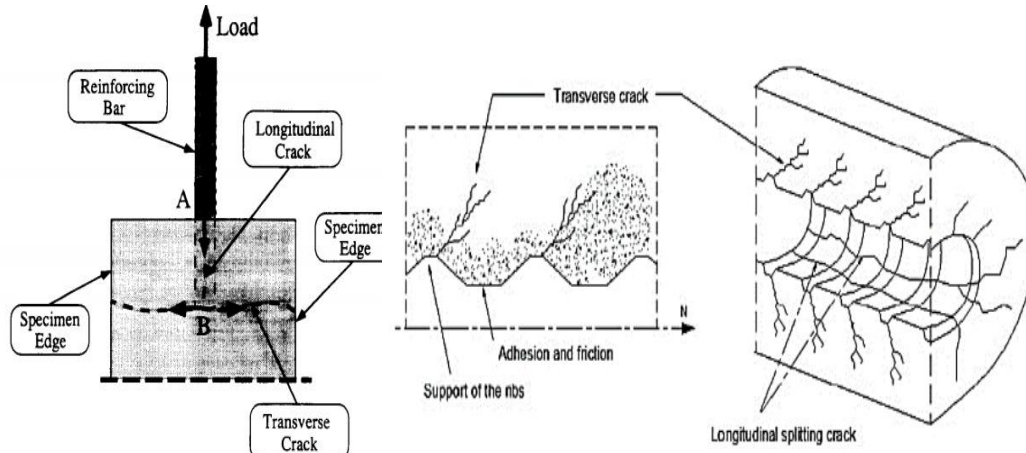


Figure 9: Comparison of the average anchorage bond strength of control and test prism specimens with GFRP reinforcing bars of diameter 12mm and 16mm at varying embedment lengths.



Figure 10: Tested double pull-out prism specimens with GFRP rebars.



(a) Krstulovic-Opara et al. [27](b)Sulaiman et al. [28]

Figure 11: Crack Pattern Propagation

5. EFFECT OF EMBEDMENT LENGTH ON THE ANCHORAGE BOND STRENGTH

Generally, the average anchorage bond strength for all the test and control specimens with end-to-end embedment of GFRP reinforcing bars increased with decreasing embedment length. However, the average anchorage bond strength values of the test specimens with 10% PKS concrete remained lower compared to that of the control specimens with NWC and GFRP reinforcing bars of diameter 12mm and 16mm as shown in Table 5 and Fig. 9. Increase in bond strength with decreasing embedment lengths were also observed by previous studies [16-20] and can be attributed to the gradual transfer of the bond stress during the pull-out test from the loaded end to the free end which results in a nonlinear stress distribution of the bond stress along the embedment length [18-20]. Conversely, the specimens with 300mm (continuous) embedment recorded the highest average anchorage bond strength values of 6.174N/mm^2 and 6.306N/mm^2 respectively for 12mm GFRP reinforcing bars in the test and control specimens and 4.581N/mm^2 and 5.584N/mm^2 respectively for 16mm GFRP reinforcing bars in the test and control specimens which can be attributed to the study by Tang [21] which reported that the maximum value on the stress distribution curve mainly occurred at or near the central anchored point, whereas the minimum value occurred at the loaded end due to the symmetry.

6. EFFECT OF BAR SIZE ON THE ANCHORAGE BOND STRENGTH

Generally, Table 5 and Fig.9 show greater anchorage bond strength for specimens with GFRP reinforcing bars of 12mm diameter compared to 16mm which is comparable to previous studies by [17, 19, 20] who also reported a reduction in bond strength values for larger GFRP reinforcing bar diameters which is attributed to an increase in the contact area between the bar and concrete as the diameter increases.

7. EFFECT OF PKS CONTENT ON THE ANCHORAGE BOND STRENGTH

The 10% PKS replacement caused a reduction in the compressive strength by 29% and 29.71% reduction in splitting tensile strength as shown in Figures 7 and 8 respectively and consequently, a reduction in the anchorage bond strength as shown in Table 5 and Fig. 9. These observations are similar to previous studies [11-15]. Alengaram et al. [14] compared the bond properties of PKSC with NWC and reported that the bond strength of PKSC was 86% of that of NWC which is in the range of (75.5-97.9%) indicated in Table 5 of this study recorded as the percentage bond strength of the NWC for the 10% PKSC.

8. FAILURE MODE AND CRACK PATTERNS

Most of the specimens shown in Fig. 10 developed longitudinal cracks that propagated from the point (A) illustrated in Figs. 11 (a) and (b) as the load was applied and towards the embedded bar end at point (B). At point (B), opening of the existing crack continues and is accompanied by the development of a transverse crack extended from point (B) toward the specimen edges. The specimen failed when the transverse crack reached the specimen edges. This pattern was noted in earlier research by Yan et al. [19] and Diab et al. [22], where splitting bond failure is extremely sudden and brittle due to the rapid production of longitudinal splitting cracks and the development of the transverse crack can be attributed to the matrix-tension failure through the net concrete section at the point of high concrete tensile stress concentration developed at the reinforcing bar end where there is a loss of most of its bond [23-25]. Similar crack patterns were observed for both test and control specimens regardless of the size of GFRP reinforcing bar and

concrete mix [19]. However, a few specimens had no visible cracks after testing. Cracks on the specimens with continuous or straight GFRP reinforcing bar embedment of 300mm had less visible cracks compared with specimens with discontinuous embedment lengths of 150mm, 125mm and 100mm which had similar and very visible cracks.

9. CONCLUSIONS

The application of GFRP reinforcing bars in LWC such as PKSC presents a unique structural material which needs to be studied. This study focused on the anchorage bond strength of Glass Fibre Polymer reinforced concrete with PKS as partial coarse aggregate. The effects of embedment length, bar size and PKS content on the anchorage bond strength were also studied and based on the test results obtained, the following conclusions are drawn:

1. Significant amount of water was absorbed by the PKS which subsequently reduced the workability of the concrete with PKS as partial coarse aggregate replacement compared with the granite in the NWC.
2. The 28 days compressive strength of the 10% PKSC was 15.79N/mm^2 which is 29% less than the 22.25N/mm^2 recorded for NWC and consequently contributed to the reduction in the anchorage bond strength.
3. The splitting tensile strength of the 10% PKSC was 1.94N/mm^2 which is 29.71% less than the 2.76N/mm^2 recorded for NWC and consequently contributed to the reduction in the anchorage bond strength.
4. Average anchorage bond strength of 4.684N/mm^2 and 3.558N/mm^2 were respectively recorded for the PKSC with 12mm and 16mm diameter bars and 100mm embedment length and 3.051N/mm^2 and 2.899N/mm^2 respectively for PKSC specimens with 12mm and 16mm diameter bars and 150mm embedment length, indicating a decrease in anchorage bond strength with increasing (end-to-end) embedment length.
5. The highest average anchorage bond strength of 6.174N/mm^2 and 4.581N/mm^2 were respectively recorded for PKSC specimens with 12mm and 16mm GFRP reinforcing bars and continuous (300mm) embedment length.

6. Comparatively, the average percentage anchorage bond strength values ranging between 75.5-97.9% of that of NWC were recorded for PKSC and an increase in GFRP reinforcing bar diameter resulted in a decrease in anchorage bond strength.
7. Splitting failure was observed for most of the specimens with longitudinal and transverse crack patterns developing after load application regardless of the size of GFRP reinforcing bar or concrete mix but the extent and visibility of the cracks formed reduced in specimens with continuous bar embedment.

COMPETING INTERESTS

The authors declare that, there are no known competing interests.

REFERENCES

- [1] Jackson N., Dhir R. K. (1996). Civil Engineering Materials (5th Edition). Palgrave. pg. 163. ISBN 978-0-333-63683-1
- [2] Chandra, S., Berntsson, L. (2003). Lightweight Aggregate Concrete – Science, Technology and Applications. Norwich, New York: William Andrew Publishing.
- [3] Teo, D.C.L., Mannan, M. A., Kurian, V. J., Ganapathy C. (2007). Lightweight concrete made from oil palm shell (OPS): structural bond and durability properties. Building and Environment, 42 (7):2614–21.
- [4] ACI 440.1R-15, Guide for the Design and Construction of Structural Concrete Reinforced with Fiber-Reinforced Polymer Bars, ACI Committee 440, 2015.
- [5] Koch G. H., Brongers M. P., Thompson N.G., Virmani Y. P., Payer J. H. (2002). Corrosion cost and preventive strategies in the United States.
- [6] Nanni, A., De Luca, A., Zadeh, H. J. (2014). Reinforced Concrete with FRP Bars: Mechanics and Design. CRC Press, Taylor and Francis Group, LLC.

- [7] Patil, G.S., Adakurkar, K., Chougule, V., Naik, S., Shitole, K., Kokate, A. (2021). Applications of Glass Fibre Reinforced Polymer (GFRP) in Concrete Structures – A review. *International Journal of Research Publication and Reviews* Vol. 2, No. 10, pp. 214-216.
- [8] Lemnitzer, L., Schröder, S., Lindorfer, A., Curbach, M. (2009). Bond behaviour between reinforcing steel and concrete under multiaxial loading conditions in concrete confinements. 20th International Conference on Structural Mechanics in Reactor Technology (SMiRT 20) Espoo, Finland, August 9-14, 2009 SMiRT 20-Division II, Paper 1734.
- [9] Bickley, J. A. (2009). A Brief History of Pullout Testing with Particular Reference to Canada-A Personal Journey Symposium Paper No. 261, Pg. 277-286 DOI: 10.14359/51663217
- [10] Buabin, T. K., Kankam, C. K., Meisuh, B. K. (2017). Bond Strength of Reinforcing Steel Bars locally milled from Scrap Metals in Concrete prepared with Palm Kernel Shell as Coarse Aggregate. *International Journal of Engineering and Technical Research (IJETR)* ISSN: 2321-0869 (O) 2454-4698 (P) Volume-7, Issue-11.
- [11] Gupta, S. K., Singh, S., Ahmad, S., Ambedkar, L. (2017). Partial Replacement of Coarse Aggregate with Palm Kernel Shell in Concrete, *International Journal of Engineering Research & Technology (IJERT)* ISSN: 2278-0181 Vol. 6 Issue 04, April-2017.
- [12] Odeyemi, S.O., Abdulwahab, R., Abdulsalama, A.A., Anifowose, M.A. (2019). Bond and Flexural Strength Characteristics of Partially Replaced Self-Compacting Palm Kernel Shell Concrete. *Malaysian Journal of Civil Engineering*, 31, 1–7.
- [13] Olanipekun, E. A., Olusola, K. O., Ata, O. (2006). A Comparative Study of Concrete Properties using Coconut Shell and Palm Kernel Shell as Coarse aggregates. *Building and Environment* 2006; 41 (3):297–301.
- [14] Alengaram, U. J., Mahmud, H., Jumaat, M. Z. (2010). Comparison of mechanical and bond properties of oil palm kernel shell concrete with normal weight concrete. *Int J Phys Sci* 2010;5(8):1231–9.
- [15] Alengaram U. J., Muhit B. A., Jumaat M. Z. (2012). Utilization of oil palm kernel shell as lightweight aggregate in concrete – A review. *Construction and Building Materials* 38 (2013), pg. 161–172.

- [16] Boateng E., Kankam C. K., Danso A. K., Ayarkwa J., Acheampong A. (2023). Bond Characteristics of Deformed Steel Rebar in Palm Kernel Shell (PKS)-Rubberised Concrete Composite. *Journal of Civil Engineering and Construction* 2023;2 (2):69-77
- [17] Wang B., Lui Gejia, Miao H. (2023). Experimental study on bond performance between Glass-Fiber-Reinforced Polymer (GFRP) bars and Concrete. *Buildings* 2023, 13(9),2126.
- [18] Shahidi, F., Wegner, L., Sparling, B. (2011). Investigation of bond between fibre-reinforced polymer bars and concrete under sustained loads. *Canadian Journal of Civil Engineering*. 33. 1426-1437. 10.1139/106-070.
- [19] Yan F., Lin Z., Yang M. (2016). Bond mechanism and bond strength of GFRP bars to concrete: A review. *Composites Part B* 98 (2016) 56-69.
- [20] Ifrahim, M.S., Sangi, A. J., Hamza S.M. (2022) Experimental Study on Bond Strength of Locally Manufactured GFRP Bar. *Eng. Proc.* 2022, 22, 4.
- [21] Tang, C.-W (2021). Modeling Uniaxial Bond Stress–Slip Behavior of Reinforcing Bars Embedded in Concrete with Different Strengths. *Materials* 2021, 14, 783.
- [22] Diab, A. M., Elyamany, H. E., Hussein, M.A., Ashy, H. M. A. (2014). Bond behavior and assessment of design ultimate bond stress of normal and high strength concrete, *Alexandria Engineering Journal* 2014; 53(2):355–371.
- [23] Di, B., Wang, J., Li, H., Zheng, J., Zheng, Y., Song, G. (2019). Investigation of Bonding Behavior of FRP and Steel Bars in Self-Compacting Concrete Structures Using Acoustic Emission Method. *Sensors (Basel)*. 2019 Jan 4; 19(1):159.doi:10.3390/s19010159.
- [24] Huang, H., Yuan, Y. J., Zhang, W., Hao, R. Q., Zeng, J. (2020). Bond properties between GFRP bars and hybrid fiber-reinforced concrete containing three types of artificial fibers. *Construction Building Materials*. 250, 18. doi:10.1016/j.conbuildmat.2020.118857.
- [25] Krstulovic-Opara, N., Watson, K. A., LaFave J. M. (1993). Effect of Increased Tensile Strength and Toughness on Reinforcing-Bar Bond Behaviour. *Cement and Concrete Composites* 16 (1994) 129-141.
- [26] Sulaiman, M.F., Ma, C.K., Apandi, N. M., Chin, S., Awang, A. Z., Mansur, S. A., Omar W. (2017). A Review on Bond and Anchorage of Confined High-strength Concrete. *Structures*, 2017 (11), pp. 97-109.

- [27] BS 882:1992, Specification for aggregates from natural sources for concrete. British Standard Institution, 2002.
- [28] Alengaram, U. J., Mahmud, H., Jumaat, M. Z., Shirazi, S. M. (2010). Effect of aggregate size and proportion on strength properties of palm kernel shell concrete. *International Journal of the Physical Sciences* 2010; 5(12):1848–1856.
- [29] Teo, D.C.L., Mannan, M. A., Kurian, V. J. (2006). Structural concrete using oil palm shell (OPS) as lightweight aggregate. *Turkish Journal of Engineering and Environmental Sciences*, 30(4):1–7.
- [30] BS EN 12390-6 (2009). Testing hardened concrete-Part 4: Tensile splitting strength of test specimens. British Standard Institution, London 2009.
- [31] ASTM D7205 (2006). Standard Test Method for Tensile Properties of Fiber Reinforced Polymer Matrix Composite Bars. ASTM Committee D30, 2006.
- [32] Kocaoz, S., Samaranayake, V., Nanni, A. (2005). Tensile characterization of glass FRP bars. *Composites Part B: Engineering* 2005; 36(2):127-134.
- [33] BS EN 12390-3 (2009). Testing hardened concrete-Part 3: Compressive strength of test specimens. British Standard Institution, London 2009.
- [34] Mannan, M. A., Ganapathy, C. (2001). Long-term strengths of concrete with oil palm shell as coarse aggregate. *Cement and Concrete Research* 2001; 31(9):1319-1321.
- [35] Okpala, D.C. (1990). Palm kernel shell as a lightweight aggregate in concrete. *Building and Environment*. 25(4):291–296.
- [36] Okafor, F. O. (1988). Palm kernel shell as a lightweight aggregate for concrete. *Cement and Concrete Research*. 18(6):901–910.
- [37] You, Y.J., Park, K.T., Seo, D.W., Hwang, J.H. (2015). Tensile Strength of GFRP Reinforcing Bars with Hollow Section. *Advances in Materials Science and Engineering*, Vol. 2015, Article ID 621546.

[38] Lui Y., Zhang H.-T., Zhao H.-H, Lu Lin, Han M.-Y, Wang J.-C, Guan S. (2021). Experimental Study on Mechanical Properties of Novel FRP Bars with Hoop Winding Layer. *Advances in Materials Science and Engineering*, vol. 2021, Article ID 9554687.

[39] Teo, D.C.L., Mannan, M. A., Kurian, V. J. (2006). Flexural behaviour of reinforced lightweight concrete beams made with oil palm shell (OPS). *Journal of Advanced Concrete Technology*, 4 (3):1–10.